

## Optical-absorption spectra of crystal-field transitions in $\text{MnPS}_3$ at low temperatures

V. Grasso, F. Neri, P. Perillo, and L. Silipigni

*Istituto di Struttura della Materia, Università degli Studi di Messina, Salita Sperone 31, Casella Postale 57, I-98166 Sant'Agata (Messina), Italy*

M. Piacentini

*Dipartimento di Energetica, Università degli Studi di Roma, La Sapienza, I-00161 Roma, Italy*

(Received 6 May 1991)

The manganese thiophosphate ( $\text{MnPS}_3$ ) optical-absorption spectrum has been investigated as a function of temperature from 300 down to 10 K in the visible region. With decreasing temperature, the fundamental absorption edge shifts towards higher energies without changing its shape and an additional subband-gap feature appears. This structure has been attributed to transitions between the  $\text{Mn}^{2+}$  third excited state and the ground state. All the subband-gap structures exhibit a small temperature shift, in good agreement both with the crystal-field theory and with the so-called transition-metal weakly interacting model. The temperature dependence of the crystal-field parameters  $Dq$ ,  $B$ , and  $C$  has been determined from the transition energies. These results support the hypothesis that  $\text{MnPS}_3$  is to be considered an ioniclike compound, as already suggested in the literature.

### I. INTRODUCTION

Recently, the manganese thiophosphates  $\text{MnPS}_3$  have received a good deal of attention because of their peculiar chemical-physical properties and their possible technological applications.<sup>1-3</sup>

A systematic analysis of the pure  $\text{MnPS}_3$  optical-absorption spectra at low temperatures, at least to our knowledge, has not been reported in the literature, even though various absorption measurements have been carried out at room temperature.<sup>4,5</sup>

Such a study is important because room-temperature measurements have the disadvantage that the internal transitions remain unresolved and are partly covered by the absorption near the direct interband gap. On the contrary, working at low temperatures allows one to resolve the details of the absorption spectra masked at room temperature by the broadening due to thermal vibrations. In this way, one obtains information on the departure of the crystal field from cubic symmetry and on the effects of the spin-orbit coupling, configuration interaction, and lattice vibrations. Moreover, the persistence of absorption at very low temperatures is an indication that transitions are partly electronically allowed.

The aim of this paper, in which we have studied the temperature dependence of  $\text{MnPS}_3$  single-crystal absorption in the visible region, is to shed light upon those structures that were not well defined in the  $\text{MnPS}_3$  room-temperature optical-absorption spectrum reported in a previous paper.<sup>4</sup>

The thermal shifts and broadenings of the observed absorption bands and the temperature variation of the  $\text{MnPS}_3$  optical band gap have also been analyzed to investigate further the nature of the involved transitions.

Moreover, the covalency amount existing in the metal-

ligand bond has been studied through the temperature dependence of the Racah  $B$  parameter, which was determined from the transition-energy position.

Both the crystal-field-theory formalism and the "transition-metal weakly interacting" model<sup>6</sup> have been used to interpret the results.

### II. EXPERIMENT

The optical-absorption spectra of  $\text{MnPS}_3$  single crystals have been obtained using a double-beam Perkin-Elmer spectrophotometer (model 330). The spectral region investigated ranged from 1.0 to 3.0 eV. Samples have been mounted in a cryostat, in which a vacuum of  $10^{-6}$  Torr has been maintained. Since the crystals were thin plates, the electric vector of the unpolarized light was perpendicular to the crystallographic  $c$  axis. All the spectra have been measured several times in order to check their reproducibility.

A cryogenerator with a two-stage cold head has been used to vary the sample temperature from 300 down to 10 K and to keep its temperature constant during each measurement run.

### III. RESULTS

A general view of the optical-absorption spectra is given in Fig. 1, where the arrows indicate the fundamental absorption-edge energy, denoted by  $E_g$  and determined through a best-fit procedure described in the following. In the region from 1.0 to 1.5 eV no absorption bands have been observed. The room-temperature absorption spectrum of such a figure shows a peak at 1.92 eV, followed by a broad shoulder at about 2.40 eV and by a sharply rising strong absorption, beginning at energies

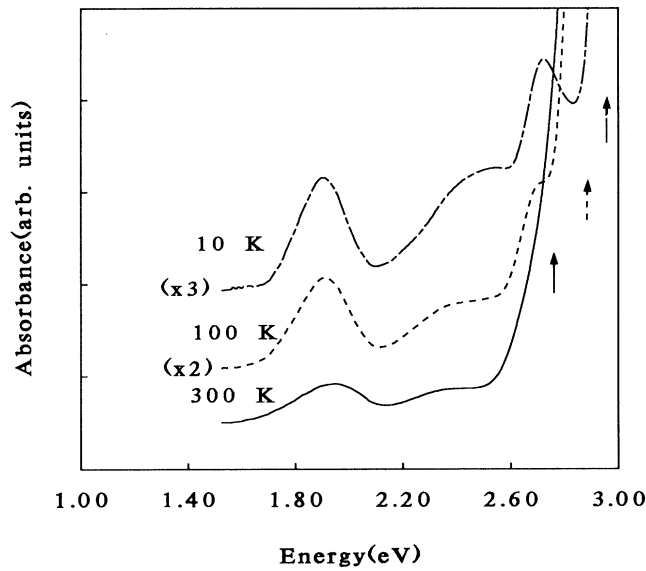


FIG. 1. Optical-absorption spectra of  $\text{MnPS}_3$  at 300, 100, and 10 K. The arrows indicate the fundamental absorption edge  $E_g$  at each temperature.

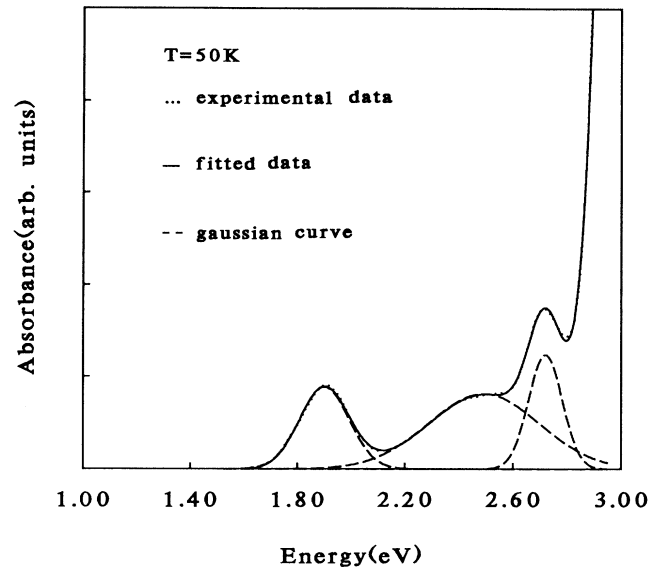


FIG. 2. Optical-absorption spectrum on  $\text{MnPS}_3$  in the region of the Mn  $3d$ - $3d$  transitions (dotted line) obtained at 50 K. The solid line is the best-fit calculated absorption spectrum, while the dashed lines are the Gaussian curves.

higher than 2.50 eV. The last covers an additional narrow band centered at about 2.64 eV, which becomes visible in the 100- and 10-K absorption spectra. In fact, by decreasing the temperature the strong absorption shifts toward higher energies without changing its shape and the third feature appears.

At each temperature no apparent substructure is present in the various bands, which are fairly well reproduced with three overlapping Gaussian curves in the lower-energy region and with an exponential function at higher energies. In Fig. 2, where the spectrum at 50 K is reported as an example, the solid line represents the best fit calculated by means of a least-squares fitting procedure, the dotted line the experimental data, and the dashed lines the obtained Gaussian curves.

In Table I the parameters values, deduced from the above fit, are reported for each temperature. The indices 1, 2, and 3 refer to the observed optical bands in order of increasing energy.

In Table II the assignments of the observed absorption structures and the fundamental absorption edge are tabulated.

The temperature variation of the fundamental absorption edge  $E_g$  is shown in Fig. 3. This threshold is seen to shift monotonically to higher energies of about 0.175 eV going from 300 to 10 K.

As shown in Fig. 1, all the subband-gap structures exhibit a temperature shift, and so we have analyzed the temperature dependence of the peaks position. Such a dependence is shown in Fig. 4, in which  $E_1$ ,  $E_2$ , and  $E_3$  represent the energy position of the observed features in order of increasing energy. In such a figure, it is possible to note that when the temperature is increased,  $E_1$  increases, while  $E_2$  and  $E_3$  decrease. Such a different behavior will be discussed in the following section.

TABLE I. Parameters values deduced from the best fit calculated by means of a least-squares fitting procedure:  $E_i$ ,  $A_i$ , and  $\sigma_i$  are, respectively, the absorption maxima energies, maxima heights, and half-widths at half maxima of the Gaussian curves used to fit the absorption bands observed in the  $\text{MnPS}_3$  optical-absorption spectra ( $i = 1, 2, 3$ , and it refers to the bands taken in order of increasing energy);  $E_g$  is the fundamental absorption edge.

$T$ (K)	$E_1$ (eV)	$E_2$ (eV)	$E_3$ (eV)	$A_1$ (a.u.)	$A_2$ (a.u.)	$A_3$ (a.u.)	$\sigma_1$ (eV)	$\sigma_2$ (eV)	$\sigma_3$ (eV)	$E_g$ (eV)
10	1.90	2.50	2.74	0.14	0.15	0.22	0.10	0.23	0.09	2.96
50	1.90	2.49	2.72	0.16	0.15	0.23	0.11	0.24	0.07	2.93
100	1.90	2.45	2.69	0.18	0.14	0.23	0.11	0.22	0.07	2.86
150	1.91	2.41	2.68	0.16	0.14	0.24	0.13	0.20	0.08	2.82
200	1.92	2.40	2.67	0.15	0.13	0.24	0.14	0.20	0.08	2.80
249	1.92	2.40	2.66	0.15	0.13	0.19	0.14	0.20	0.08	2.80
300	1.92	2.40	2.64	0.15	0.13	0.26	0.15	0.18	0.09	2.79

TABLE II. Assignments of the observed absorption structures and fundamental absorption edge, whose energy positions are denoted  $E_1$ ,  $E_2$ ,  $E_3$ , and  $E_g$ , respectively, are indicated.

	Position (eV) (10–300 K)	Assignment
$E_1$	1.90–1.92	${}^6A_{1g} \rightarrow {}^4T_{1g}$
$E_2$	2.50–2.39	${}^6A_{1g} \rightarrow {}^4T_{2g}$
$E_3$	2.74–2.67	${}^6A_{1g} \rightarrow \{ {}^4E_g, {}^4A_{1g} \}$
$E_g$	2.96–2.79	${}^6A_{1g} \leftarrow P, S \ 3p_x p_y$

#### IV. DISCUSSION AND ASSIGNMENT OF THE TRANSITIONS

It is well known that transition-metal-compound absorption spectra can be interpreted in terms of both transitions involving the electrons in the incomplete outer  $d$  shell of the transition-metal ion, called “crystal-field” transitions, and in terms of excitations, usually more intense and farther out in the ultraviolet, of electrons from the ligands to the metal (or the reverse), known as “change-transfer” transitions.

Bearing this in mind and making reference to existing literature,<sup>4–7</sup> we will restrict the structure assignments to these cases. Such a choice is in good agreement with the so-called transition-metal weakly interacting model,<sup>6</sup> which regards the  $d$  electrons as localized and not participating in bonding. This model has been successfully used in the interpretation of the  $\text{MnPS}_3$  room-temperature optical-absorption, fluorescence, and reflectivity spectra and of the  $\text{MnPS}_3$  electrical transport properties.<sup>4,8–10</sup>

In the  $\text{MnPS}_3$  compound the five  $d$  orbitals, degenerate in the free ion, are split by the octahedral field, imposed by the ligands (sulfur atoms), into a triply degenerate set of  $d_e$  orbitals, corresponding to the representation  $t_{2g}$  in

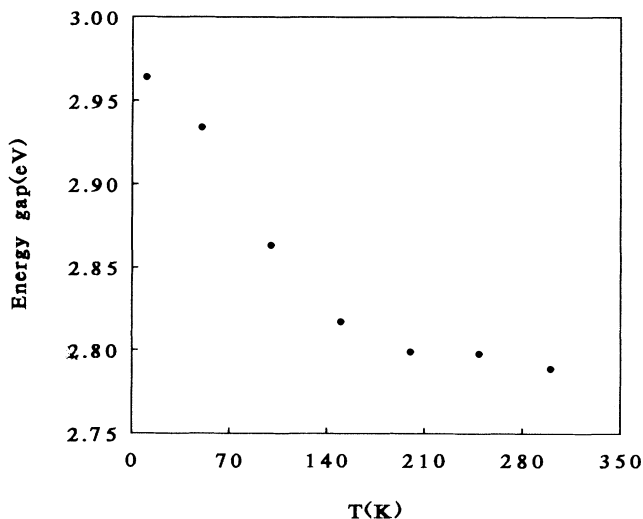


FIG. 3. Temperature dependence of the  $\text{MnPS}_3$  fundamental absorption edge  $E_g$  (see Table I).

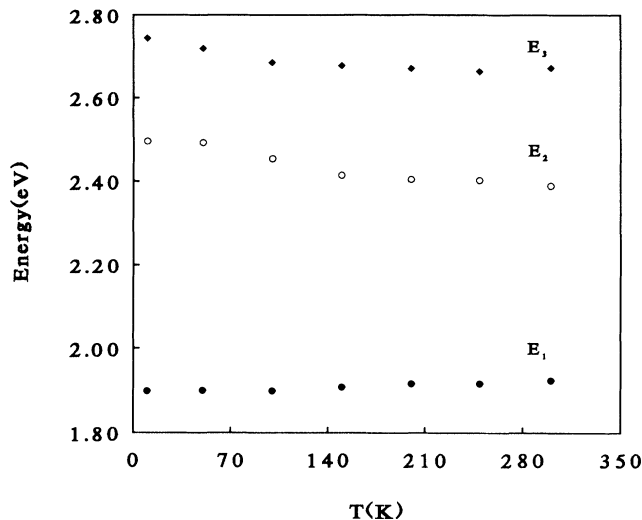


FIG. 4. Temperature dependence of the observed optical-absorption features energy position.  $E_1$ ,  $E_2$ , and  $E_3$  represent the  ${}^6A_{1g} \rightarrow {}^4T_{1g}$ ,  ${}^6A_{1g} \rightarrow {}^4T_{2g}$ , and  ${}^6A_{1g} \rightarrow \{ {}^4E_g, {}^4A_{1g} \}$  transitions energy, respectively (see Table II).

Mullikan notation,<sup>11</sup> and into a doubly degenerate set of  $d\gamma$  orbitals whose Mullikan representation is  $e_g$ .<sup>12</sup>

For negatively charged anions arranged at the corners of a regular octahedron, as happens in  $\text{MnPS}_3$ , the  $e_g$  orbitals are higher in energy than the  $t_{2g}$  orbitals and the energy difference between the  $e_g$  and  $t_{2g}$  orbitals,  $\Delta$ , is set equal, by convention, to  $10Dq$  (with  $Dq > 0$ ),<sup>13</sup> following a notation reported in the literature.<sup>14</sup> Such a difference is therefore given in terms of two quantities  $D$  and  $q$ , which are simply combined into a single semiempirical parameter  $Dq$  in such a geometry. The quantity  $D$ , wholly connected with the ligands, is usually called the field parameter since it is an index of the field strength exerted on the central ion by the ligands, while the quantity  $q$  is a measure of the effect of the cubically arranged charges on the radial wave function of the central metal ion.<sup>11</sup>

In the  $\text{Mn}^{2+}$  free ion, the lowest-lying electronic level is a  ${}^6S$  arising from the configuration  $3d^5$ , which also gives rise to  ${}^4G$ ,  ${}^4P$ ,  ${}^4D$ , and  ${}^4F$  terms above the ground level. When the  $\text{Mn}^{2+}$  ion is in a crystal, the ground state is not affected by the cubic field,<sup>12,15</sup> while the quartet levels are split by the influence of the surrounding ions immediately adjacent to the transition-metal ion (the ligands). This is the case with  $\text{MnPS}_3$ , for which the  $\text{Mn}^{2+}$  ground state is  ${}^6A_{1g}(S)$ , which has the orbital configuration  $(t_{2g}^3 e_g^2)$  with five unpaired spins. The free-ion  ${}^4G$  state is split by the octahedral field into two triply degenerate states  ${}^4T_{1g}(G, t_{2g}^4 e_g^1)$  and  ${}^4T_{2g}(G, t_{2g}^4 e_g^1)$ , a doubly degenerate state  ${}^4E_g(G, t_{2g}^3 e_g^2)$ , and a nondegenerate state  ${}^4A_{1g}(G, t_{2g}^3 e_g^2)$ . These are the first four  $\text{Mn}^{2+}$  excited states.

Among these quartet levels, the  ${}^4E_g(G)$  and  ${}^4A_{1g}(G)$  ones are degenerate in absence of any distortion of the octahedral field. They have the same orbital configuration

as the ground state and are not affected by low-symmetry components of the crystal field. On the other hand, the  ${}^4T_{1g}(G)$  and  ${}^4T_{2g}(G)$  levels, which have an orbital configuration unlike that of the ground state, are influenced by such fields only via configurational mixing to a first-order approximation.<sup>16</sup>

Since the energy levels are determined mainly by the crystal field, with the aid of the energy-level diagram, calculated by Orgel for the  $Mn^{2+}$  ion,<sup>17</sup> it is possible to assign the observed bands to certain transitions.

Thus the three structures observed in the room-temperature optical-absorption spectrum at about 1.92, 2.40, and 2.64 eV can be ascribed to the transitions from the  ${}^6A_{1g}$  ground state to the quartet  ${}^4T_{1g}$ ,  ${}^4T_{2g}$ , and  $\{{}^4E_g, {}^4A_{1g}\}$  excited states (the notation  $\{ \}$  means that the two levels are degenerate). These transitions are sextet-quartet intercombinations, and therefore the spin-selection rule  $\Delta S = 0$  must be broken since these spin-dependent interactions involve a change in multiplicity. In the free space, they are forbidden as electric dipole processes because all states of the  $d$  shell have the same parity. However, being the probability of a magnetic dipole transition approximately weaker by a factor of  $(137)^2$  than the electric dipole transition, even a small breakdown in the parity-selection rule allows the electric dipole transitions to appear and dominate.<sup>18</sup> This accounts for why the  ${}^6A_{1g} \rightarrow \{{}^4E_g, {}^4A_{1g}\}$  and  ${}^6A_{1g} \rightarrow {}^4T_{2g}$  transitions are more intense than the  ${}^6A_{1g} \rightarrow {}^4T_{1g}$  excitation. Moreover, these transitions are allowed in  $MnPS_3$  because, in the bidimensional approximation, adopted in the transition-metal weakly interacting model, the  $MnPS_3$  crystal symmetry is represented by the  $D_{3d}$  space group. The presence of such a symmetry causes these excitations, with either  $xy$  or  $z$  polarization, to become allowed.<sup>18-20</sup>

Since from previous optical data<sup>4-7</sup> we know that the  $MnPS_3$  compound is predominantly ionic, the  $3d$  levels energies will depend on the  $Dq$ ,  $B$ , and  $C$  parameters. In fact, in a purely ionic picture, the energy levels for  $d$  electrons in octahedral cubic fields depend not only on the crystal-field parameter  $\Delta$  (or  $10Dq$ ), but also on the values of the Coulomb and exchange integrals describing the electrostatic repulsion between the  $d$  electrons. These integrals are expressed in terms of the Racah parameters  $B$  and  $C$ , whose ratio is nearly constant, namely,  $\gamma = C/B = 4.5$ , for all ions of the transition series.<sup>21</sup> Thus we can express the  $Mn^{2+}$  ion  ${}^4T_{1g}$ ,  ${}^4T_{2g}$ , and  $\{{}^4E_g, {}^4A_{1g}\}$  excited states energies as follows:

$$\begin{aligned} (t_2^4 e^1) \begin{cases} E[{}^4T_1] = -10Dq + 10B + 6C - 26B^2/10Dq \\ E[{}^4T_2] = -10Dq + 18B + 6C - 38B^2/10Dq \end{cases}, & (1) \\ (t_2^3 e^2) E[{}^4E, {}^4A_1] = 10B + 5C, & \end{aligned}$$

while the  $Mn^{2+}$   ${}^6A_{1g}(S, t_2^3 e^2)$  ground-state energy is set equal to zero.<sup>22</sup>

Since the  $Mn^{2+}$  ground state is independent of the crystal field<sup>23</sup> and it is usually close to its equilibrium configuration, the  $3d-3d$  transitions take place to a variety of vibrational levels of the excited states in accordance with the Frank-Condon principle.<sup>24</sup> The tempera-

ture behavior of a band is therefore substantially related to that of the involved excited state. In particular, as temperature is changed, some subband-gap structures ( ${}^4T_{1g}$  and  ${}^4T_{2g}$  bands) show a thermal broadening due to two possible mechanisms:<sup>24</sup> (i) a transfer of energy from the ionic system to the phonon bath, which is accomplished simultaneously by the electric transition, and (ii) a temperature-independent, inhomogeneous contribution to the bandwidths, which becomes evident at low temperature at which the thermal vibrations are quenched and is due to microscopic strains in crystals, which, being randomly spaced, produce a Gaussian shape.

The first effect, that is, the interaction with the lattice thermal vibrations, can consist in Raman scattering of phonons by the  $Mn^{2+}$  ion, as observed for several transition-metal ions.<sup>24</sup>

In the following sections the temperature behavior of each  $MnPS_3$  optical-absorption structure will be discussed in detail.

#### A. ${}^6A_{1g}(S, t_2^3 e_g^2) \rightarrow {}^4T_{1g}(G, t_2^4 e_g^1)$ transition (band 1)

This is an interconfigurational transition, that is,

$$t_2^n e^m \rightarrow t_2^{n-k} e^{m+k}, \quad (2)$$

with  $k = -1$ . Such an excitation is broad compared to that between  ${}^6A_{1g}$  and  $\{{}^4E_g, {}^4A_{1g}\}$  states since it involves states of different orbital electronic configuration. In fact, since the  $e_g$  orbitals are  $\sigma$  antibonding and the  $t_{2g}$  orbitals practically nonbonding, a change in the electron distribution between them results in a change in the equilibrium metal-ligand distance and therefore in the equilibrium configuration of the local environment. As a result of the action of the Franck-Condon principle, such a change gives rise to a broadening of the spectrum.<sup>21</sup>

As the temperature increases, the band maximum shifts to a higher frequency and a slight broadening can be observed (see Figs. 1 and 4 and Table I). The thermal shift should reflect the changes of the crystal field with temperature. In fact, referring to the energy-level diagram given by Orgel<sup>17</sup> (where the lowest quartet-levels energies, relative to the ground state, are given as a function of the crystal-field strength  $Dq$ ), we can relate the temperature dependence of the peak energy position to the strong  ${}^4T_1$  dependence on  $Dq$ . This statement can be explained as follows.

The parameter  $Dq$  is a temperature function according to the equation

$$Dq \propto \frac{c}{R^n}, \quad (3)$$

where  $c$  is a constant determined by the transition-metal ion and ligands,  $R$  is the distance between the absorbing center ( $Mn^{2+}$  ion) and ligands (sulfur atoms), and the exponent  $n$  is equal to 5 in the charge model or 6 in the dipole model.

On the other hand,  $R$  being a function of temperature through the thermal-expansion coefficient  $\alpha$  of the material, that is

$$R(T) = R(0)(1 + \alpha T), \quad (4)$$

Eq. (3) becomes

$$Dq \propto \frac{c}{[R(0)]^n(1+\alpha T)^n} \approx \frac{c}{[R(0)]^n}(1-n\alpha T). \quad (5)$$

Such an expression asserts that  $Dq$  decreases when the temperature increases; that is, a crystal expansion reduces the strength of the crystalline field and changes the transition frequency, which, therefore, depends on temperature. Such an implicit dependence can be expressed, for each crystal configuration  $t_{2g}^m e_g^{n-m}$  (where  $n$  is the total number of  $d$  electrons in the ion; for instance, for  $Mn^{2+}$ ,  $n = 5$ ), by

$$E = h\nu = aDq, \quad (6)$$

where  $a = (6n - 10m)$ . In particular, for  ${}^4T_{1g}$ , whose configuration is  $t_{2g}^4 e_g^1$ , we obtain  $a = -10$ . This negative value explains well the  $E_1$  shift toward higher energies on increasing temperature (see Fig. 4 and Table I).

#### B. ${}^6A_{1g}(S, t_{2g}^3 e_g^2) \rightarrow {}^4T_{2g}(G, t_{2g}^4 e_g^1)$ transition (band 2)

This is also an interconfigurational transition such as the  ${}^6A_{1g} \rightarrow {}^4T_{1g}$  excitation. In the energy-level diagram given by Orgel,<sup>17</sup> the  ${}^4T_{2g}$ -level energy depends on  $Dq$  less than the  ${}^4T_{1g}$ -level energy. Moreover, such a level shows an exceptionally strong configurational mixing with the  ${}^4T_2(D, t_{2g}^3 e_g^2)$  level due to either spin-orbit or Coulomb interactions, which slightly reduces the electron-phonon interaction.<sup>25</sup>

On decreasing the temperature, the band peak shifts toward higher energies and both the bandwidth and amplitude increase (see Fig. 4 and Table I). Such a band shows therefore an opposite behavior of that of the  ${}^4T_1$  band even if the  ${}^4T_{1g}$  and  ${}^4T_{2g}$  states have the same orbital electronic configuration. The different behavior of the  ${}^4T_{2g}$  level seems due to the appreciable configurational mixing of the level with the upper  ${}^4T_{2g}(D)$  one in analogy to some compounds, such as  $MnBr_2$  and  $MnCl_2$ .<sup>25</sup>

#### C. ${}^6A_{1g}(S, t_{2g}^3 e_g^2) \rightarrow \{{}^4E_g, {}^4A_{1g}\}(G, t_{2g}^3 e_g^2)$ transition (band 3)

The transition to these quasidegenerate levels is quite interesting because of its intraconfigurational character. It is sharp compared to those excitations involving states of different orbital configuration.

In the Orgel energy-level diagram,<sup>17</sup> the energy of such degenerate levels, relative to the ground state, does not depend on  $Dq$ , but it is due to the electrostatic interaction between the  $d$  electrons, and therefore it can be expressed through the Racah  $B$  and  $C$  coefficients as shown in the third equation of Eqs. (1).

At room temperature this transition is covered by the strong absorption to the high-energy side of the second band. As the temperature decreases, the band peak, attributed to this transition, appears and shifts to higher energies (Figs. 1 and 4).

Since the position of the degenerate levels  $\{{}^4E_g, {}^4A_{1g}\}$  is not affected by changes in the crystal field brought by

TABLE III. Values of the  $B$ ,  $C$ , and  $Dq$  parameters for the  $Mn^{2+}$  ion contained in  $MnPS_3$  at 10, 50, and 100 K.

$T$ (K)	$B$ ( $cm^{-1}$ )	$C$ ( $cm^{-1}$ )	$Dq$ ( $cm^{-1}$ )
100	632	3066	813
50	683	3020	814
10	684	3058	843

the lattice vibrations [see the third equation of Eqs. (1)], it should not shift with temperature if the Racah parameters  $B$  and  $C$  are constant.<sup>26</sup> But the energy of a crystal-field-independent transition is not necessarily independent of the totally symmetric motion of the ligands, as the covalency factors vary with metal-ligand overlap and, hence, with the metal-ligand distance. So, using Eqs. (1), we have calculated the  $Dq$ ,  $B$ , and  $C$  values at 100, 50, and 10 K, that is, at those temperatures at which the structures were better defined. These values are listed in Table III.

We have observed some trends in the experimentally deduced values of  $Dq$ ,  $B$ , and  $C$ : the  $Dq$ ,  $B$ , and  $C$  parameters are not constant; in particular,  $B$  and  $Dq$  decrease as the temperature increases. The  $Dq$  temperature dependence is consistent with crystal-field theory for which a crystal expansion would reduce the strength of the crystalline field. The decrease in  $B$  is ascribed to an increase in covalency amount existing in the metal-ligand bonds of  $MnPS_3$ ,<sup>4,8</sup> in analogy with the  $B$  behavior of some covalent compounds.<sup>27</sup>

With the aid of the Koide-Pryce curves,<sup>28</sup> in which the variation of the  ${}^4E_g$ - and  ${}^4A_{1g}$ -level energies as function of the covalency parameter  $\epsilon$  is shown, we have found an  $\epsilon$  value of about 0.175 at 10 K and about 0.185 at 300 K, observing an increase in covalency when temperature increases.

Since, differently from the  ${}^4T_{1g}$  and  ${}^4T_{2g}$  levels, the positions of the levels  ${}^4E_g({}^4G)$  and  ${}^4A_{1g}({}^4G)$  depend only on the covalency parameter  $\epsilon$ ,<sup>29</sup> the temperature dependence of the  $\{{}^4E_g, {}^4A_{1g}\}$  degenerate levels can be assigned to a covalency variation.

The shift of the band peak toward lower energies, as the temperature increases (curve  $E_3$  of Fig. 4), agrees with the work of Koide and Pryce, in which the increasing covalency of the Mn compounds results in the energy lowering and splitting of these originally degenerate levels.

#### D. $S\ 3p_x p_y$ band $\rightarrow {}^6A_{1g}$ charge-transfer transition

Figure 1 shows that the steeply rising edge of the  $MnPS_3$  absorption shifts toward higher energies with decreasing temperature without changing its shape. The position of the band edge corresponds approximately to that deduced for  $MnPS_3$  from previous optical-absorption data by Brec *et al.*<sup>5</sup>

In the extrema ionic picture, because of their localization on the transition-metal ion, the  $Mn^{2+}\ 3d$  states, split by the octahedral field, lie in the gap of the P  $p_z$  bonding-antibonding bands. The  $MnPS_3$  valence bands derive from the sulfur  $3s, 3p_x p_y$ , and from the phosphorus

$3s, 3p_z$  bonding states of the  $(P_2S_6)^{4-}$  cluster. In our experimental geometry, with the light incident at near-normal incidence on the basal plane, i.e., with  $xy$  polarization, the transitions involving the  $P p_z$  bonding-antibonding bands are dipole forbidden. Hence the observed sharply rising strong absorption is due to the charge-transfer transition from the  $S 3p_x p_y$  bands to the  $Mn^{2+} 3d$  ground state, that is, to a valence-band-localized-state transition.

In analogy to other semiconductor compounds, the effects which give rise to the observed fundamental absorption edge thermal shift can be (i) the thermal-expansion effect or what is often called the "dilation contribution," which accounts for the effect of the change of lattice constant on the energy gap producing a shift in the relative position of the conduction and valence bands, or (ii) the "constant-volume electron-phonon scattering" due to the interaction between the ionic system and normal modes of lattice vibrations setup, at the ion site, by the crystalline field, which varies in time with the thermal vibrations of neighboring ions.

All this can be expressed as follows:

$$\begin{aligned} \frac{\delta E_g}{\delta T} &= \left( \frac{\delta E_g}{\delta T} \right)_{\text{epn}} + \left( \frac{\delta E_g}{\delta T} \right)_{\text{ph}} \\ &= \frac{\alpha}{\beta} \left( \frac{\delta E_g}{\delta P} \right)_T + \left( \frac{\delta E_g}{\delta T} \right)_{\text{ph}}, \end{aligned} \quad (7)$$

where the expansion coefficient  $\alpha$  is equal to  $(1/V)(\delta V/\delta T)_P$  and the compressibility  $\beta$  is equal to  $-(1/V)(\delta V/\delta P)_T$ .<sup>30</sup>

The first term is expected since the electronic energy bands are formed because of the overlappings of electronic wave functions, the extent of which is dependent upon the distances between neighboring atoms or ions.<sup>31</sup>

With respect to the second term, its magnitude is often very much greater than the first, and with only a few exceptions, its existence has been treated in the literature in a phenomenological way.<sup>32</sup>

Since no data on the  $\alpha$ ,  $\beta$ , and  $(\delta E_g/\delta P)_T$  coefficients are available for  $MnPS_3$ , we cannot determine the first term of Eq. (7), and consequently no choice between these two interpretations can be made on the basis of our experimental data. Nevertheless, making reference to existing literature, it is possible to give a qualitative interpretation of the observed temperature  $E_g$  behavior. In fact, as reported in the literature<sup>33</sup> the phenomenon, observed

in other compounds, has been attributed to the thermal expansion, noting, however, that this effect is too small to account for the observed shift. Radkowsky, indeed, has assigned such a shift to a broadening of the electron levels due to collisions with thermally vibrating lattice, which results in reducing the effective width of the forbidden-energy region.<sup>33</sup>

Adopting the latter hypothesis and bearing in mind that the  $Mn^{2+} 6A_{1g}$  ground state is insensitive to changes in the crystal field brought about by lattice vibrations, we can think that the shift is due to a broadening of the  $S 3p_x p_y$  band due to collisions with the thermally vibrating lattice. So, increasing the temperature, the upper limit of the  $S 3p_x p_y$  band comes close to the  $Mn^{2+}$  ground state and the  $E_g$  value decreases.

## V. CONCLUSIONS

The temperature dependence of the  $MnPS_3$  single-crystal optical absorption has been studied with particular attention to the  $Mn^{2+} 3d$  levels, which seem to play no significant role in bonding. In the investigated temperature range, the structures, observed below the fundamental threshold, have been assigned to  $Mn^{2+} 3d-3d$  transitions on the basis of crystal-field theory. It is shown that a temperature variation produces a shift of the energy position of both the structures and optical band gap. In particular, the shift of the fundamental absorption edge makes clearly visible a third  $3d-3d$  transition, whose existence was inferred, in previous room-temperature measurements, only through the second derivation of the spectrum itself.

Using crystal-field theory and the transition-metal weakly interacting model, some important remarks have been made about the each structure temperature dependence: (i) the  ${}^4T_{1g}$ -band maximum shift is related to the strong  ${}^4T_{1g}$  dependence on  $Dq$ , (ii) the  ${}^4T_{2g}$ -band peak shift is due to the appreciable configurational mixing of this level with the upper  ${}^4T_{2g}(D)$  one, (iii) the shift of the  $\{{}^4E_g, {}^4A_{1g}\}$ -band peak is assigned to a variation in covalency amount existing in the metal-ligand bonds of  $MnPS_3$  (such a change is confirmed by the temperature behavior of the Racah  $B$  coefficient), and (iv) the fundamental absorption-edge thermal shift is ascribed to a broadening of the  $S 3p_x p_y$  band due to collisions with the thermally vibrating lattice.

<sup>1</sup>R. Brec, G. Ouvrard, A. Louisy, and J. Rouxel, *Solid State Ion.* **6**, 185 (1982).

<sup>2</sup>R. Brec, D. M. Schleich, A. Louisy, G. Ouvrard, and J. Rouxel, *Inorg. Chem.* **18**, 1814 (1979).

<sup>3</sup>A. Le Mehaute, G. Ouvrard, R. Brec, and J. Rouxel, *J. Mater. Res. Bull.* **12**, 1191 (1977).

<sup>4</sup>V. Grasso, S. Santangelo, and M. Piacentini, *Solid State Ion.* **20**, 9 (1986).

<sup>5</sup>R. Brec, D. Schleich, A. Louisy, and J. Rouxel, *Ann. Chim. (Fr.)* **3**, 347 (1978).

<sup>6</sup>M. Piacentini, F. S. Khumalo, C. G. Olson, J. W. Anderegg, and D. W. Lynch, *Chem. Phys.* **65**, 289 (1982).

<sup>7</sup>M. Piacentini, F. S. Khumalo, G. Leveque, C. G. Olson, and D. W. Lynch, *Chem. Phys.* **72**, 61 (1982).

<sup>8</sup>V. Grasso, F. Neri, L. Silipigni, and M. Piacentini, *Phys. Rev. B* **40**, 5529 (1989).

<sup>9</sup>V. Grasso, F. Neri, L. Silipigni, and M. Piacentini, *Nuovo Cimento D* **13**, 633 (1991).

<sup>10</sup>V. Grasso, F. Neri, S. Santangelo, L. Silipigni, and M. Piacentini, *J. Phys. Condens. Matter* **1**, 3337 (1989).

- <sup>11</sup>Physical Chemistry, *An Advanced Treatise*, edited by H. Eyring (Academic, New York, 1970), Vol. V, Chap. V.
- <sup>12</sup>G. M. Barrow, *Introduction to Molecular Spectroscopy* (McGraw-Hill, New York, 1962), p. 293.
- <sup>13</sup>C. J. Ballhausen, *Introduction to Ligand Field Theory*, *McGraw-Hill Series in Advanced Chemistry* (McGraw-Hill, New York, 1962).
- <sup>14</sup>J. W. Stout, *J. Chem. Phys.* **31**, 709 (1959).
- <sup>15</sup>H-h. Chou and H. Y. Fan, *Phys. Rev. B* **10**, 901 (1974).
- <sup>16</sup>R. Pappalardo, *J. Chem. Phys.* **33**, 613 (1960).
- <sup>17</sup>L. E. Orgel, *J. Chem. Phys.* **23**, 1004 (1955).
- <sup>18</sup>M. Tinkham, *Group Theory and Quantum Mechanics* (McGraw-Hill, New York, 1964), Chap. 4.
- <sup>19</sup>R. Engleman, *The Jahn-Teller Effect in Molecules and Crystals* (Wiley-Interscience, London, 1972), p. 302.
- <sup>20</sup>L. D. Landau and E. M. Lifshitz, *Quantum Mechanics*, Vol. 3 of a *Course of Theoretical Physics* (Pergamon, London, 1959), Chap. 12.
- <sup>21</sup>D. McClure, in *Solid State Physics*, edited by F. Seitz and D. Turnbull (Academic, New York, 1959), Vol. 9, p. 499.
- <sup>22</sup>N. B. Hannay, in *Treatise on Solid State Chemistry*, edited by N. B. Hannay (Plenum, New York, 1975), Vol. II.
- <sup>23</sup>L. E. Orgel, *J. Chem. Phys.* **23**, 1824 (1955).
- <sup>24</sup>B. Di Bartolo, *Optical Interactions in Solids* (Wiley, New York, 1986), Chap. 17.
- <sup>25</sup>I. Pollini, G. Spinolo, and G. Benedek, *Phys. Rev. B* **22**, 6369 (1980).
- <sup>26</sup>J. C. Zahner and H. G. Drickamer, *J. Chem Phys.* **35**, 1483 (1961).
- <sup>27</sup>D. L. Wood, in *Optical Properties of Solids*, edited by S. Nudelman and S. S. Mitra (Plenum, New York, 1969), Chap. 19, p. 576.
- <sup>28</sup>S. Koide and M. H. L. Pryce, *Philos. Mag.* **3**, 607 (1958).
- <sup>29</sup>J. W. Stout, *J. Chem. Phys.* **33**, 303 (1960).
- <sup>30</sup>M. L. Cohen and D. J. Chadi, in *Handbook on Semiconductors*, edited by T. S. Moss (North-Holland, Amsterdam, 1980), Vol. II.
- <sup>31</sup>Y. F. Tsay, B. Gong, S. S. Mitra, and I. F. Vetalino, *Phys. Rev. B* **6**, 2330 (1972).
- <sup>32</sup>J. Tauc, in *Proceedings of the International School of Physics "Enrico Fermi,"* Course XXXIV, edited by J. Tauc (Academic, New York, 1966).
- <sup>33</sup>A. Radkowsky, *Phys. Rev.* **73**, 749 (1948).